

PAPER • OPEN ACCESS

## Can lubricant oil promote undesired self-ignition of the charge in hydrogen engines?

To cite this article: E. Distaso *et al* 2023 *J. Phys.: Conf. Ser.* **2648** 012084

View the [article online](#) for updates and enhancements.

You may also like

- [Preparation of microcapsules containing double-component lubricant and self-lubricating performance of polymer composites](#)  
Haiyan Li, Nanqi Shi, Jing Ji et al.
- [Oil viscosity effects on lubricant oil film behaviour under minimum quantity lubrication](#)  
N E H Zamiruddin, A S A Sani and N Rosli
- [Nanopore-based electrokinetic purification of oil-in-water emulsions with temperature and pH modulation](#)  
Qin Zeng, Dequan Xu, Wenbo Wu et al.

**PRIME**  
PACIFIC RIM MEETING  
ON ELECTROCHEMICAL  
AND SOLID STATE SCIENCE

HONOLULU, HI  
Oct 6-11, 2024

Abstract submission deadline:  
**April 12, 2024**

Learn more and submit!

**Joint Meeting of**  
The Electrochemical Society  
•  
The Electrochemical Society of Japan  
•  
Korea Electrochemical Society

# Can lubricant oil promote undesired self-ignition of the charge in hydrogen engines?

E. Distaso\*, G. Calò, R., Amirante, D. A. Baloch, P. De Palma, P. Tamburrano

Department of Mechanics, Mathematics and Management, Politecnico di Bari, Italy

\* Corresponding author's e-mail: elia.distaso@poliba.it

**Abstract.** Hydrogen utilization in internal combustion engines is deemed a viable solution for promoting a rapid transition towards a carbon-free mobility, especially for those hard-to-electrify applications. However, critical aspects still poorly understood remain and need to be investigated in order to accelerate the development of such a promising technology. Some of these might originate from the undesired but unavoidable participation of lubricant oil to the combustion process. The present work aims at ascertaining if the lubricant oil chemical characteristics can be at the basis of the onset of certain uncontrolled self-ignition modes of the charge. Considering a lubricant oil droplet suspended in a  $H_2/air$  environment, an analytical model was developed to derive essential information about mixture composition and thermodynamic conditions that might establish where oil contamination occurs. The results were used to initialize zero-dimensional numerical simulations performed in the OpenSMOKE++ framework with the aim of highlighting charge reactivity variations induced by the presence of oil vapour in the vicinity of an oil droplet. A reduced chemical model, developed for this very purpose in a previous recent work, was employed in the simulations for emulating the reactivity properties of the  $H_2/oil/air$  mixture.

## 1. Introduction

Hydrogen has regained attention in response to the urgent need of abandon fossil fuels due to the adverse impact that greenhouse gas emissions from the transportation sector are producing on the climate. The scientific research in the field of Internal Combustion Engines (ICEs) has continued to produce innovation in the last few decades for further developing this propulsion system. New combustion techniques [1,2] and architectures [3–5] coupled with new strategies for controlling the combustion process [6–8] and more accurate and cost-effective sensors [9–11] have been proposed. However, in order to still consider ICEs a sustainable option for the future, the attention needs to be necessarily shifted on the fuels used for feeding the system [12,13]. Hydrogen can give new possibilities of development to ICEs, by replacing fossil fuels in those applications in which the battery-based technologies are still not mature.

Although hydrogen is one of the most studied fuels, there exist criticalities that need to be addressed for rendering hydrogen ICEs ready for the marketplace [14–16]. Among these, there is the uncontrolled spontaneous premature ignition of the charge, which reduces the combustion control, limits the engine power output and forces the operation in very lean conditions in order to avoid potential engine failure [16,17]. The onset of some abnormal combustion modes that arise even in the absence of any significant charge or temperature inhomogeneity might rely on the presence of lubricant oil contamination within the combustion chamber. Fundamental research showed that a relative short alkane molecule like n-



heptane can increase the reactivity of  $H_2/air$  mixtures in the low-temperature range even by more than one order of magnitude [18]. Considering that the main components of base oils are normal alkanes having a number of carbon atoms ranging from 15 to 54 [19], lubricant oil results considerably more reactive than n-heptane and might have more pronounced effects on the reactivity of  $H_2/air$  mixtures.

Evidence linking the presence of lubricant oil inside the combustion chamber to particularly severe detonation phenomena is already reported in the literature in the case of highly boosted gasoline engines, especially at low speeds and high loads [20,21]. Lubricant oil significantly accelerates gasoline ignition [22,23], and, in the case of hydrogen, the effects might be even more relevant, bearing in mind the larger difference in the molecular structure existing between hydrogen and lubricant oil, in comparison to that existing between gasoline and lubricant oil. Recent works on hydrogen ICEs have started to link the onset of abnormal combustions to the presence of “sensitive spots” whose generation has been ascribed to lubricant oil contamination [17,24,25].

It is worth to mention that there is also a secondary pathway by which lubricant oil can interfere with the regular evolution of the combustion process. Lubricant oil can represent a significant source of nano-sized soot particles, as observed in recent experiments [26–29], since the formation of soot precursor species is facilitated in the case of the long-chain hydrocarbons constituting lubricant oil [30,31]. When carbonaceous deposits are formed, these can serve as additional sensitive spots, able to initiate an uncontrolled ignition of the charge [21].

Understanding the reaction pathways involved in the oxidation of lubricant oil and its interaction with hydrogen could play a crucial role in the development of efficient and reliable hydrogen ICEs. Some useful information can already be inferred from previous research even though mainly oriented to gasoline engines [32–38]. Namely, a common approach consists in the use of a single n-alkane molecule, i.e., n-hexadecane ( $n-C_{16}H_{34}$ ), as a surrogate species for emulating lubricant oil chemical characteristics [34–36,38].

On the basis of this same hypothesis, a reaction mechanism was developed in a recent previous work [39] for studying the reactivity behaviour of  $H_2/n-C_{16}H_{34}/air$  mixtures in what can be considered the first attempt to characterize the effects induced by the interaction of hydrogen with lubricant oil. It was found that lubricant oil can significantly increase the charge reactivity, especially in the low-temperature range. The results showed that lubricant oil surrogate species remains highly more reactive than  $H_2$  for a wide range of temperatures, as it can be observed in Figure 1, which is reported as an example for the reader’s convenience (observe the existence of regions 2 and 3). This result pointed out that the presence of lubricant oil can facilitate the mixture ignition at temperatures considerably lower than those at which hydrogen usually auto-ignites (at a given pressure). In [39] several  $H_2/n-C_{16}H_{34}/air$  mixtures having different compositions were analysed as well, highlighting that very small amounts of lubricant oil are sufficient to promote the auto-ignition of the charge. However, those analyses did not provide information about the effective amounts of lubricant oil that can be found where oil contamination occurs, namely in the vicinity of oil droplets.

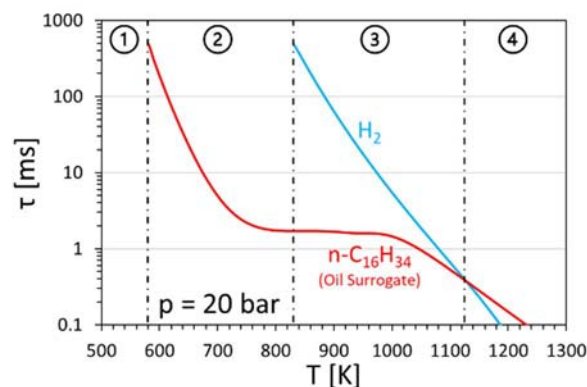


Figure 1. Results obtained in [39] regarding the ignition behaviour of  $n-C_{16}H_{34}/air$  and  $H_2/air$  mixtures at a pressure of 20 bar and an equivalence ratio of 0.5.

The aim of the present work is to find out if a lubricant oil droplet suspended in a  $H_2/air$  environment can effectively represent a sensitive spot from which a chemical process can start and propagate throughout the charge. To this purpose, a relatively simple analytical model is developed to derive reasonable profiles of the temperature and the mass fraction around the droplet. The results were used to initialize zero-dimensional numerical simulations performed in the OpenSMOKE++ framework. n-hexadecane was selected as a surrogate chemical species to model the chemical and physical behaviour of lubricant oil and the reduced chemical model, developed in [39] was employed in the simulations for emulating the reactivity properties of  $H_2/oil/air$  mixtures. With this approach it was possible to study the charge reactivity variations induced by the presence of oil vapour in the vicinity of an oil droplet, providing quantitative information with small computational efforts.

## 2. Analytical Model

Modelling the vaporization of a liquid oil droplet in an environment consisting of hydrogen and air is not a trivial task. The mathematical description of the heat and mass transfer processes involves complex partial differential equations that are usually solved through numerical integration techniques, when a detailed description of the related physical processes is required. However, the present work does not aim at providing a comprehensive description of the evaporating behaviour of an oil droplet, but, more practically, it is rather focused on the attempt of highlighting the potential threat to the regular engine operation constituted by the  $H_2/oil/air$  gaseous mixture that forms around an oil droplet.

The present analytical model was conceived with the aim of obtaining expressions for the temperature and species distributions in the region close to the droplet surface, with a limited computation effort, but which result physically reasonable, so that they could be used to initialize reactive 0D numerical simulations. With this approach it was possible to assess the spatial variation of the mixture ignition delay time, induced by the oil droplet without the need of performing complex and time demanding CFD simulations. Despite its simplicity, this analytical model gives useful information that, coupled with chemical analyses, can provide useful insight in the problem.

### 2.1. Model description

As depicted in Figure 2, the model considers a single droplet existing in a quiescent, infinite medium constituted by a  $H_2/air$  mixture and in which a temperature higher than that of the droplet reigns. A spherically symmetric coordinate system was employed for describing the problem, in which the radius,  $r$ , is the only coordinate variable and has its origin at the centre of the droplet. The variables at the liquid-vapor interface are denoted with the subscript “s”. Energy necessary to vaporize the liquid is transferred, in the form of heat, from the surrounding ambient to the droplet, and, simultaneously, the oil vapor diffuses from the droplet surface into the ambient gas. The interactions with any other droplets, and the effects of convection are ignored. Radiation heat transfer is considered negligible. The pressure is considered uniform and constant. The lubricant oil droplet is a single-component liquid, with zero solubility for gases and having the n-hexadecane properties. The evaporation process is considered to be much slower than the involved chemistry, so that, a quasi-steady assumption is used to describe the process. The thermodynamic parameters, such as the gas-phase thermal conductivity,  $\lambda$ , and specific heat,  $c_{p,g}$ , as well as the product of the density and mass diffusivity,  $\rho\mathcal{D}$ , are all considered constants. The hypothesis of unit Lewis number,  $Le = \lambda / (c_{p,g}\rho\mathcal{D})$ , is invoked.

With the above assumptions, the oil (n-hexadecane) mass fraction distribution  $Y_{oil}(r)$  and the temperature distribution  $T(r)$  in the gaseous ambient surrounding the droplet can be found by solving the gas-phase mass, species and energy conservation equations, the droplet gas-phase interface energy balance, and the droplet liquid mass conservation equation.

From the gas-phase mass conservation, with the assumption of quasi-steady vaporization, it can be stated that the mass flowrate,  $\dot{m}$ , is a constant, independent of the radius, thus:

$$\dot{m} = 4\pi r^2 \rho v = 4\pi r^2 \rho_s v_s = const, \quad (1)$$

where  $v$  is the velocity of the flow leaving the droplet surface.

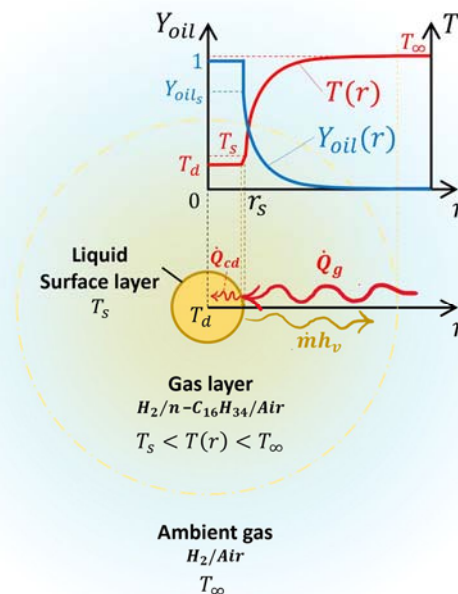


Figure 2. Schematization of the evaporation process according to the "onion skin" model, enclosing energy fluxes at the surface and the expected mass fraction,  $Y_{oil}(r)$ , and Temperature,  $T(r)$ , distributions.

It is possible to obtain an expression describing how the n-hexadecane concentration varies moving away from the droplet surface by solving the steady species conservation equation, which can be written as

$$\frac{d}{dr}(4\pi r^2 \rho v Y_{oil}) = \frac{d}{dr}\left(4\pi r^2 \rho D \frac{dY_{oil}}{dr}\right). \quad (2)$$

For the vaporizing droplet, the total mass flow rate leaving the droplet surface must be equal to the sum of the mass flow rates due to the bulk convective motion of gaseous mixture at the surface and the mass diffusion rate of the vapour in the radial direction due to the existence of a concentration gradient around the droplet surface. Considering that the total flowrate is everywhere identical to the oil vapour flowrate, the condition to which the species conservation equation must be constrained can be expressed as

$$\rho_s v_s = \left[\rho v Y_{oil} - \rho D \frac{dY_{oil}}{dr}\right]_s. \quad (3)$$

Equation (2) can be integrated two times with respect to  $r$ , by imposing the condition expressed by Equation (3) and that  $Y_{oil} = Y_{oil_s}$  at the surface (where  $r = r_s$ ). After some algebra, it is possible to find the expression that describe the n-hexadecane concentration variation along the radial coordinate, viz.,

$$Y_{oil}(r) = 1 - \frac{(1 - Y_{oil_s}) e^{-\frac{Z}{r}}}{e^{-\frac{Z}{r_s}}}, \quad (4)$$

where  $Z = \frac{1}{4\pi D \rho}$ . The unity Lewis number assumption implies that  $\frac{\lambda}{c_{p,g}} = \rho D$ , thus the parameter  $Z$  can be also expressed as  $Z = \frac{c_{p,g}}{4\pi \lambda}$ .

The temperature distribution in the gas phase can be obtained as a solution of the gas-phase energy conservation equation, which, with the  $Le = 1$  assumption, reduces to the simple Shvab–Zel'dovich form

$$4\pi r^2 \rho v \frac{d(c_{p,g} T)}{dr} = \frac{d}{dr}\left[4\pi \frac{\lambda}{c_{p,g}} r^2 \frac{d(c_{p,g} T)}{dr}\right]. \quad (5)$$

Assuming that the gas-phase thermal conductivity,  $\lambda$ , and specific heat,  $c_{p,g}$ , are constant, Equation (5) can be integrated twice with respect to  $r$ , by imposing the boundary conditions far from the droplet surface, i.e.,  $T = T_\infty$  for  $r \rightarrow \infty$ , and at the droplet surfaces, i.e.,  $T = T_s$  for  $r = r_s$ , as illustrated in Figure 2. The temperature distribution in the gas phase can be then obtained:

$$T(r) = \frac{(T_\infty - T_s)e^{-\frac{Z\dot{m}}{r}} - T_\infty e^{-\frac{Z\dot{m}}{r_s}} + T_s}{1 - e^{-\frac{Z\dot{m}}{r_s}}}. \quad (6)$$

In order to evaluate the mass species and temperature distributions, it is necessary to calculate the evaporation rate,  $\dot{m}$ , by writing the energy balance at the droplet surface. Figure 2 schematizes the instantaneous energy fluxes at the surface of the evaporating droplet. The gas-phase ambient is at a higher temperature than the droplet, so that heat ( $\dot{Q}_g$ ) is conducted through the gas phase and transferred to the droplet surface. This energy is that required to heat up the liquid ( $\dot{Q}_{cd}$ ) and induce the oil vaporization ( $\dot{m}\Delta_v h_{oil}$ ). Mathematically, this can be expressed as

$$\dot{Q}_g = \dot{m} \Delta_v h_{oil} + \dot{Q}_{cd}, \quad (7)$$

where  $\Delta_v h_{oil}$  is the heat of vaporization of the oil. The instantaneous conduction heat transfer from the gas phase,  $\dot{Q}_g$ , can be evaluated by applying Fourier's law, while the instantaneous heat conducted into the droplet interior,  $\dot{Q}_{cd}$ , can be easily evaluated by employing the so-called "onion-skin" model, which considers the droplet as consisting of an interior region existing uniformly at its initial temperature,  $T_d$ , and a thin liquid surface layer at the surface temperature,  $T_s$ . In this model,  $\dot{Q}_{cd}$  in Equation (7) represents the thermal power required to heat the fuel from  $T_d$  to  $T_s$ . With these assumptions, Equation (7) can be rewritten as

$$\left[ \lambda 4\pi r^2 \frac{dT}{dr} \right]_s = \dot{m} [\Delta_v h_{oil} + c_{p,l}(T_s - T_d)] \quad (8)$$

where  $c_{p,l}$  is the specific heat of the liquid n-hexadecane, and the temperature gradient at the interface can be obtained from the temperature distribution in the gas layer around the droplet (Equation (6)). After some algebra it is possible to write an expression that links the evaporation mass flow rate,  $\dot{m}$ , to the droplet surface temperature,  $T_s$ , namely,

$$\dot{m} = \frac{r_s}{Z} \ln \left[ 1 + \frac{c_{p,g}(T_\infty - T_s)}{\Delta_v h_{oil} + c_{p,l}(T_s - T_d)} \right] = \frac{r_s}{Z} \ln[1 + B], \quad (9)$$

where  $B = \frac{c_{p,g}(T_\infty - T_s)}{\Delta_v h_{oil} + c_{p,l}(T_s - T_d)}$  represents the transfer number for this specific problem.

In addition to the evaporation rate,  $\dot{m}$ , Equations (4) and (6) require the knowledge of the n-hexadecane mass fraction and temperature values at the droplet surface, namely,  $Y_{oil_s}$  and  $T_s$ , respectively.

It is possible to evaluate the n-hexadecane concentration at the droplet surface as a function of the mass flow rate,  $\dot{m}$ , by imposing to Equation (4) the condition that  $Y_{oil} = 0$  for  $r \rightarrow \infty$ , namely, no oil present in the  $H_2/air$  mixture far away from the droplet:

$$Y_{oil_s} = \frac{B}{B + 1}. \quad (10)$$

A relation between  $Y_{oil_s}$  and  $T_s$  that provide closure to the problem can be obtained by assuming equilibrium between the liquid and vapor phases at the droplet surface. Such an equilibrium can be described in a simple form by employing the Clausius–Clapeyron equation, which links the partial pressure of oil (n-hexadecane) vapor at the liquid-vapor interface,  $p_{oil_s}$ , at a given temperature,  $T_s$ , to the vapor pressure estimated in a known reference state, i.e.,

$$\frac{p_{oil_s}}{p_{oil_s,ref}} = e^{-\frac{\Delta_v h_{oil}}{R} \left( \frac{1}{T_s} - \frac{1}{T_{s,ref}} \right)}, \quad (11)$$

where, and  $T_{s,ref}$  is the boiling temperature of lubricant oil (n-hexadecane) at the reference pressure  $p_{oil_s,ref}$  (1 atm). The oil vapour partial pressure,  $p_{oil_s}$ , can be related to the oil mole fraction,  $\chi_{oil_s}$ , and mass fraction,  $Y_{oil_s}$ , as follows:

$$Y_{oil_s} = \frac{p_{oil_s}}{p} \frac{MW_{oil}}{\chi_{oil_s} MW_{oil} + (1 - \chi_{oil_s}) MW_{\infty}}, \quad (12)$$

where  $MW_{oil}$  and  $MW_{\infty}$  are the molecular mass of the oil (n-hexadecane) and the average molecular mass of the  $H_2/air$  mixture far from the droplet, respectively.

Substituting Equation (12) into Equation (11) yields an explicit relation between  $Y_{oil_s}$  and  $T_s$ , namely,

$$Y_{oil_s} = \frac{e^{-\frac{\Delta_v h_{oil}}{R} \left( \frac{1}{T_s} - \frac{1}{T_{s,ref}} \right)} MW_{oil}}{e^{-\frac{\Delta_v h_{oil}}{R} \left( \frac{1}{T_s} - \frac{1}{T_{s,ref}} \right)} MW_{oil} + \left[ p - e^{-\frac{\Delta_v h_{oil}}{R} \left( \frac{1}{T_s} - \frac{1}{T_{s,ref}} \right)} \right] MW_{\infty}}. \quad (13)$$

Equations (9), (10) and (13) can be solved simultaneously in order to evaluate the conditions at the droplet surface, namely in order to obtain  $\dot{m}$ ,  $Y_{oil_s}$  and  $T_s$ . These values can be used to evaluate the mass fraction distribution  $Y(r)$  and the temperature distribution  $T(r)$  in the gaseous ambient surrounding the droplet, using Equations (4) and (6), respectively.

## 2.2. Parameters estimation

In order to evaluate the derived equations, a proper selection of appropriate mean values for the liquid- and gas-phase thermodynamics properties of the involved species and mixtures was needed.

The specific heat of liquid n-hexadecane,  $c_{p,l}$ , was evaluated by means of the polynomial expression provided by Zhang et al. [40], at the temperature of the liquid droplet,  $T_d$ , namely,

$$c_{p,l} = c_{p,l}^{oil}(T_d) = a_1 + a_2 T_d + a_3 T_d^2, \quad (14)$$

with the coefficients reported in Table 1.

For the gas-phase specific heat,  $c_{p,g}$ , and the thermal conductivity,  $\lambda$ , in the gas layer surrounding the droplet, the approach suggested by Law and Williams [41] was employed. i.e., the gas-phase specific heat,  $c_{p,g}$ , was approximated with that of oil vapours, namely, with that of gaseous n-hexadecane,  $c_{p,g}^{oil}$ , as

$$c_{p,g} = c_{p,g}^{oil}(\bar{T}); \quad (15)$$

while the gas-phase thermal conductivity value was evaluated as a weighted average with respect to the value of gaseous n-hexadecane,  $\lambda_g^{oil}$ , and that of the  $H_2/air$  mixture,  $\lambda_{\infty}$ , [41] as

$$\lambda(\bar{T}) = 0.4 \lambda_g^{oil}(\bar{T}) + 0.6 \lambda_{\infty}(\bar{T}). \quad (16)$$

The characteristic temperature,  $\bar{T}$ , at which these parameters were evaluated, was estimated via the so-called ‘‘one-third rule’’ [42], namely,

$$\bar{T} = T_s + \frac{(T_{\infty} - T_s)}{3}. \quad (17)$$

The gas-phase specific heat value at  $\bar{T}$  was evaluated by means of the following polynomial expression:

$$c_{p,g}^{oil}(\bar{T}) = \frac{R}{MW_{oil}} (a_1 + a_2 \bar{T} + a_3 \bar{T}^2 + a_4 \bar{T}^3 + a_5 \bar{T}^4), \quad (18)$$

Table 1 Coefficients employed in the polynomial expressions for the specific heat of liquid n-hexadecane,  $c_{p,l}^{oil}(T_d)$  [40]; for the specific heat,  $c_{p,g}^{oil}(\bar{T})$  [39] and thermal conductivity,  $\lambda_g^{oil}(\bar{T})$  [43] of gaseous n-hexadecane.

	$a_1$	$a_2$	$a_3$	$a_4$	$a_5$	$a_6$	$a_7$	$a_8$
$c_{p,l}^{oil}$	[J/(Kg K)]	[J/(Kg K <sup>2</sup> )]	[J/(Kg K <sup>3</sup> )]					
	1720.2	-0.53	$6 \cdot 10^{-3}$					
$c_{p,g}^{oil}$	[-]	[1/K]	[1/K <sup>2</sup> ]	[1/K <sup>3</sup> ]	[1/K <sup>4</sup> ]			
	$-3.64 \cdot 10^0$	$0.196 \cdot 10^0$	$-1.27 \cdot 10^{-4}$	$4.14 \cdot 10^{-8}$	$-5.41 \cdot 10^{-12}$			
$\lambda_g^{oil}$	[W/(mK)]	[W/(mK)]	[W/(mK)]	[W/(mK)]	[W/(mK)]	[W/(mK)]	[W/(mK)]	[-]
	4.25547	-39.3553	140.965	-244.669	143.418	-48.4488	6.8884	0.152925

Table 2 Coefficients employed in the polynomial expression for the thermal conductivity,  $\lambda_i(T)$  of the considered species.

Ref.	[44]	[44]	[45]
	N <sub>2</sub>	O <sub>2</sub>	H <sub>2</sub>
$a_1$ [W/(mK)]	$-8.14736 \cdot 10^{-4}$	$6.85176 \cdot 10^{-4}$	101.93
$a_2$ [W / (mK <sup>2</sup> )]	$1.1613984 \cdot 10^{-4}$	$9.39908 \cdot 10^{-5}$	0.3081
$a_3$ [W / (mK <sup>3</sup> )]	$-1.1361924 \cdot 10^{-7}$	$-2.44914 \cdot 10^{-8}$	$4 \cdot 10^{-5}$
$a_4$ [W / (mK <sup>4</sup> )]	$1.0617612 \cdot 10^{-10}$	$4.31987 \cdot 10^{-12}$	0
$a_5$ [W / (mK <sup>5</sup> )]	$-5.4055704 \cdot 10^{-14}$	0	0
$a_6$ [W / (mK <sup>6</sup> )]	$1.4542066 \cdot 10^{-17}$	0	0
$a_7$ [W / (mK <sup>7</sup> )]	$-1.941557 \cdot 10^{-21}$	0	0
$a_8$ [W / (mK <sup>8</sup> )]	$1.0105922 \cdot 10^{-25}$	0	0

in which R is the universal gas constant ( $R = 8314.5 \text{ J/kmol K}$ ), and the coefficients were the same used in the thermodynamic dataset of the reaction mechanism [39], and are reported in Table 1.

For the gaseous n-hexadecane thermal conductivity value at  $\bar{T}$ , the polynomial expression suggested by Monogenidou et al. [43], validated in conditions varying from the triple point to 700 K and up to 50 MPa, was employed:

$$\lambda_g^{oil}(\bar{T}) = \frac{a_1 - a_2 T_r + a_3 T_r^2 - a_4 T_r^3 + a_5 T_r^4 - a_6 T_r^5 + a_7 T_r^6}{a_8 - T_r}, \quad (19)$$

where  $T_r = \bar{T}/T_c^{oil}$ , represents the ratio between the characteristic temperature  $\bar{T}$  and the n-hexadecane critical temperature,  $T_c^{oil} = 722 \text{ K}$  [40]. The relative coefficients are reported in Table 1, as well.

The thermal conductivity of the  $H_2$ /air gas mixture constituting the ambient in which the oil droplet is suspended,  $\lambda_\infty$ , was evaluated by employing the widespread used empirical correlation proposed by Mathur et al. [46], also in accordance with the suggestion provided in a recent review work by Zhukov et al. [47] about the calculation of thermal conductivity of gas mixture containing hydrogen. Known the mixture composition expressed in terms of mole fractions,  $\chi_i$ , the average thermal conductivity can be calculated as

$$\lambda_\infty(\bar{T}) = \frac{1}{2} \left[ \sum_i \chi_i \lambda_i + \left( \sum_i \frac{\chi_i}{\lambda_i} \right)^{-1} \right]. \quad (20)$$

For the thermal conductivity of the  $i$ -th species (with  $i = H_2, N_2, O_2$ ) constituting the ambient gas mixture,  $\lambda_i$ , the following general polynomial expression was employed:

$$\lambda_i = \lambda_i(\bar{T}) = a_1 + a_2 \bar{T} + a_3 \bar{T}^2 + a_4 \bar{T}^3 + a_5 \bar{T}^4 + a_6 \bar{T}^5 + a_7 \bar{T}^6 + a_8 \bar{T}^7. \quad (21)$$

The thermal conductivity of nitrogen, oxygen and hydrogen were evaluated using the polynomial coefficient values suggested by Abramenko et al. [44] and by Bergman et al. [45] respectively, validated

in a range spanning from 80 K to 4500 K for nitrogen, from 100 to 2500 K for oxygen and from 400 K to 2000 K for hydrogen. The relative values are reported in Table 2. Finally, the n-hexadecane boiling temperature at reference atmospheric conditions,  $T_{s,ref}$ , was selected equal to 560 K and the molar heat of vaporization,  $\Delta_v h_{oil} = 51.84 \text{ KJ/mol}$  at  $T_{s,ref}$  [48].

### 2.3. Boundary conditions

A lubricant oil droplet can have a diameter ranging from 0.01 to 3.0 mm, according to literature data obtained through high speed images [49]. Increasing longer induction times before ignition have been observed for droplets having increasing larger sizes [50,51]. Wang et al. [50] showed that the ignition delay time of an oil droplet having a radius of 200  $\mu\text{m}$  was about 200 ms under operating conditions of 20 bar and 780 K. Considering that an ICE for automotive applications needs significantly less than 200 ms to cover one entire compression stroke, probably, a droplet radius smaller than 100  $\mu\text{m}$  is required to trigger an auto-ignition event. Consequently, three different oil droplet sizes were selected for this study, namely,  $r_s = 25, 50$  and 75  $\mu\text{m}$ .

A temperature of the liquid in the inner region of the droplet,  $T_d$ , equal to 423 K was imposed, considering that oil droplets are usually released from the piston crevice due to the piston motion [52]. Thus, the temperature at which the oil is released should not differ much from that of the cylinder liner, which is usually lower than 500 K.

The thermo-chemical conditions of the ambient in which the oil droplet is suspended were selected in order to resemble typical conditions reigning within the combustion chamber of an ICE just before that the piston reaches the TDC, namely when undesired pre-ignitions of the charge are usually detected [50,53]. Three ( $p, T_\infty$ ) values pairs were selected to analyse different scenarios, namely,  $p = 30 \text{ bar}$  and  $T_\infty = 800\text{K}$ ,  $p = 50 \text{ bar}$  and  $T_\infty = 900\text{K}$ ,  $p = 70 \text{ bar}$  and  $T_\infty = 1000\text{K}$ . These conditions might be interpreted as either different piston locations along the last part of the compression stroke of the same engine or different thermodynamic conditions obtained with different engine architectures (compression ratios). The analyses were carried out at three different values of the fuel equivalence ratio of the  $H_2/air$  mixture surrounding the oil droplet,  $\phi_\infty$ , namely, 0.25, 0.5 and 0.75.

### 3. Numerical simulations set-up

The results obtained from the analytical model were used to initialize 0D numerical simulations performed within the open-source OpenSMOKE++ framework [54] and having the aim to quantify the ignition delay time variation along the radial coordinate,  $\tau(r)$ . The closed homogeneous batch reactor model with constant volume assumption was employed for solving the time dependent balance equations for the total mass, the gas-phase species mass and energy. A criterion for the ignition delay time evaluation based on the maximum OH increase was used. The reduced reaction mechanism developed in a previous study [39] for  $H_2/n-C_{16}H_{34}/air$  mixtures and consisting of 169 species and 2796 reaction was employed in the simulations. The 1D spatial domain employed in the computations with the analytical model was discretized using 50 points, distributed according to a spacing criterion based on 5 K temperature increment of the  $T(r)$  function. The same values for  $p$ ,  $T_\infty$  and  $\phi_\infty$ , considered in the calculations performed with the analytical model were considered for the numerical simulations.

### 4. Results and Discussion

Figure 3 reports the profiles of mass fraction,  $Y_{oil}(r)$  (blue lines) and temperature,  $T(r)$  (red lines) obtained from the analytical model, in correspondence of the three droplet radii,  $r_s$ , considered, namely 25  $\mu\text{m}$  (dotted lines), 50  $\mu\text{m}$  (dashed lines) and 75  $\mu\text{m}$  (solid lines). The corresponding ignition delay profile,  $\tau(r)$  (green lines), obtained from the 0D simulations, is reported for each condition in the bottom graph. Figure 3 refers to ambient conditions of  $T_\infty = 900 \text{ K}$ ,  $p = 50 \text{ bar}$ , and  $\phi_\infty = 0.5$ . The variables are plotted against the radial distance from the droplet centre in Figure 3 (a), while the dimensionless distance from the droplet surface  $\delta = (r - r_s)/r_s$  is considered in Figure 3 (b). The latter shows that the results scale with the droplet radius, as expected with the hypothesis at the basis of the model.

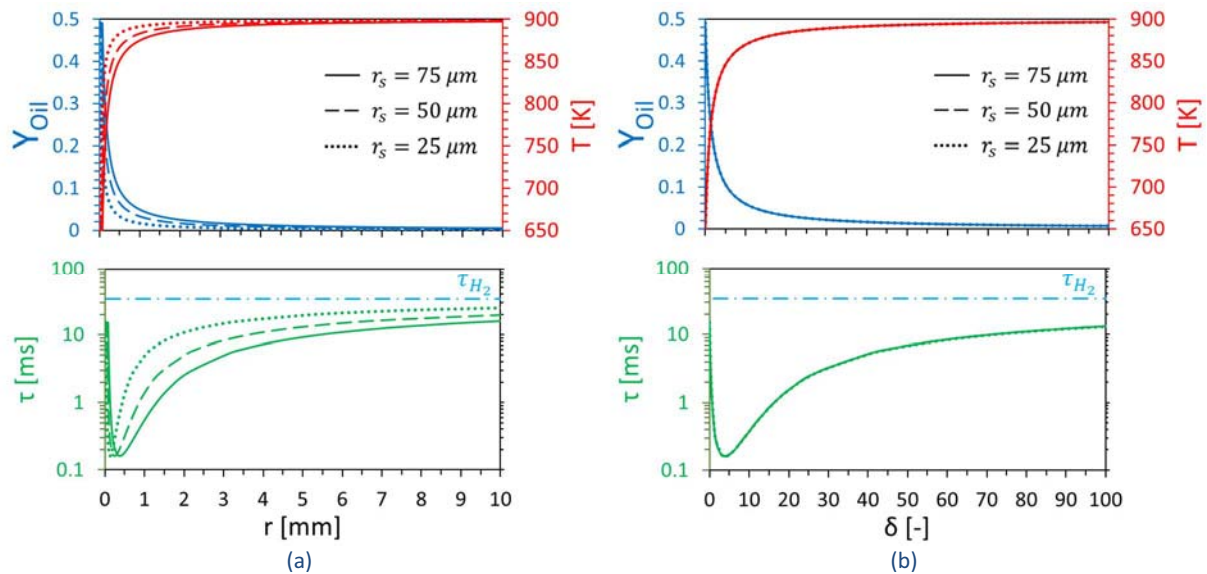


Figure 3. Mass fraction,  $Y_{oil}$ , and temperature,  $T$ , distributions obtained from the analytical model, together with ignition delay time distributions,  $\tau$ , obtained from the 0D simulations, for three different droplet radii (25, 50 and 75  $\mu\text{m}$ , at ambient conditions of  $T_\infty = 900\text{ K}$ ,  $p = 50\text{ bar}$ ,  $\phi_\infty = 0.5$ ). The functions are plotted both against the radial coordinate,  $r$  (a) and the dimensionless distance,  $\delta$  (b).

The main result is that  $\tau(r)$  remains much lower than the reference value of the  $H_2/air$  mixture at the ambient conditions ( $\tau_{H_2}$  light blue line) even at a significant distance from the droplet, regardless of the droplet size. Namely, in the thermo-chemical conditions of Figure 3, the  $H_2/air$  mixture would require about 34 ms to ignite, whereas, even at a distance equal to 100 droplet radii (where  $Y_{oil}$  is decreased to about 0.007) the  $H_2/oil$  mixture needs less than 15 ms. This suggests that the gas layer that surrounds the droplet represents an extremely high-reactive region that extends significantly far from its surface, and that even trace amounts of lubricant oil are sufficient to significantly increase the charge reactivity.

The oil mass fraction at the droplet interface,  $Y_{oil,s}$ , never exceeds a value of 0.5 (mainly due to the high ambient pressure) and moving away from the droplet,  $Y_{oil}(r)$  quickly decreases, so that, at a distance equal to 5 droplet radii, its value is already less than 0.1. The temperature has an opposite trend, namely,  $T(r)$  starts from a value at the droplet interface,  $T_s$ , of about 650 K, and quickly increases reaching a value of about 835 K after 5 droplet radii. Near the droplet surface, although very rich conditions are established, the temperature remains close to that of the liquid and significantly lower than that of the ambient, so that the chemical process is slowed down. Far from the droplet, the oil vapour concentration decreases drastically and with it the effects on the reactivity. As a consequence, the  $\tau(r)$  function, shows a minimum located at a distance comprised between 2 and 12 droplet radii, range in which  $\tau$  remains shorter than 0.5 ms, as can be more clearly observed in Figure 4, which reports a closer view of the values obtained in the proximity of the droplet surface.

Although a low temperature ( $T_s \approx 650\text{ K}$ ) and a quite significant mixture enrichment, the mixture obtained close to the droplet interface show high reactivity, with an ignition delay value that is more than halved ( $\tau_s \approx 15\text{ ms}$ ) in comparison to the reference value reached at infinite distance from the droplet ( $\tau_\infty \equiv \tau_{H_2} \approx 34\text{ ms}$ ). However, the ignition will probably start at the distance of about 4 droplet radii, where a minimum value of about 0.16 ms is recorded. It is worth to highlight that this ignition delay value is more than 2 orders of magnitude shorter than the hydrogen reference value,  $\tau_{H_2}$ . As a reference, at this temperature (and pressure) the  $H_2/air$  mixture would require more than 100 ms to ignite (depending on the equivalence ratio considered).

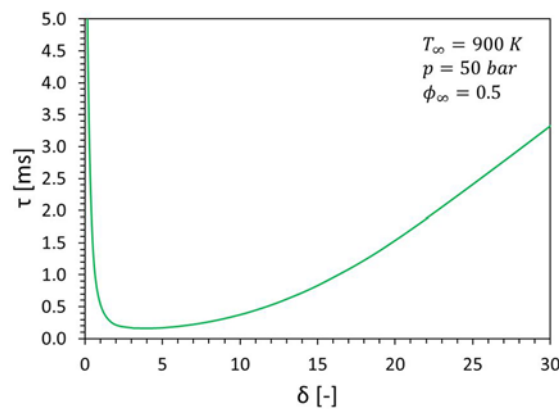


Figure 4. Ignition delay time,  $\tau(\delta)$ , variation close to the droplet surface at ambient conditions of  $T_\infty = 900\text{ K}$ ,  $p = 50\text{ bar}$ ,  $\phi_\infty = 0.5$ .

The extent of the effects induced by lubricant oil contamination on the charge reactivity changes depending on the thermo-chemical conditions of the ambient in which the oil droplet is suspended. Figure 5 (a) shows the results deriving from the calculations made at three different conditions in terms of ambient temperature and pressure, and in which the equivalence ratio,  $\phi_\infty$ , was kept constant at a value of 0.5. Although the temperature is increased from 800 to 1000 K, the oil mass fraction does not vary much from one case to another. This is because the pressure was increased simultaneously with the temperature in the considered cases. The trend recorded for  $\tau$  is similar to that shown in Figure 3 for all the considered cases, but with some peculiarities that is worth examining.

At 800 K and 30 bar, the thermodynamic conditions are not suitable for promoting the  $H_2/air$  mixture autoignition. Nevertheless, the  $\tau(\delta)$  profile (green dotted line in Figure 5 (a)) shows a deep through, analogously to the other reactive cases. This means that the presence of an oil droplet has the potential to drastically shift the explosion limit of hydrogen, by generating a highly reactive mixture during its vaporization even in condition in which hydrogen would not auto-ignite. At a distance of about 5 radii, the formed  $H_2/oil/air$  mixture needs only about 1 ms to auto-ignite, and  $\tau(\delta)$  remains shorter than 10 ms up to a distance equal to 25 radii. This is a remarkable finding, if one considers that a spontaneous ignition of the charge could be locally initiated by an oil droplet even though the thermodynamic conditions are considered safe for the operation of a hydrogen engine.

At 1000 K and 70 bar, the  $H_2/air$  mixture would require about 2.5 ms to auto-ignite. With the presence of an oil droplet, this time can be reduced to about 60  $\mu\text{s}$  at a distance slightly lower than 5 droplet radii (cf. solid lines in Figure 5 (a)), highlighting a maximum reduction of about 98% induced by the oil vapour at the highest ambient temperature and pressure considered.

A less marked dependence upon the ambient equivalence ratio arose from the results showed in Figure 5 (b), in which  $T_\infty = 900\text{ K}$  and  $p = 50\text{ bar}$  were considered. This suggests that the lubricant oil effects are significative, independently of the hydrogen content in the charge. The increased reactivities is mainly attributable to the low-temperature chemistry involved in the long straight-chain alkanes oxidation, in which the  $H_2-O_2$  system play a quite marginal role [39,51]. The minimum value of  $\tau$  is about 0.15 ms and it is recorded at approximately 4.5 radii, for all the conditions considered. It is meaningful to point out that the ignition delay shortening induced by lubricant oil is much more pronounced than that induced by an increase in the equivalence ratio value of the  $H_2/air$  mixture. Namely,  $\tau_{H_2}$ , changes approximately from 53 to 26 ms, when  $\phi_\infty$  is increased from 0.25 to 0.75 (cf. light blue lines in Figure 5 (b)), while the reduction induced by the oil contamination can reach up to two orders of magnitude.

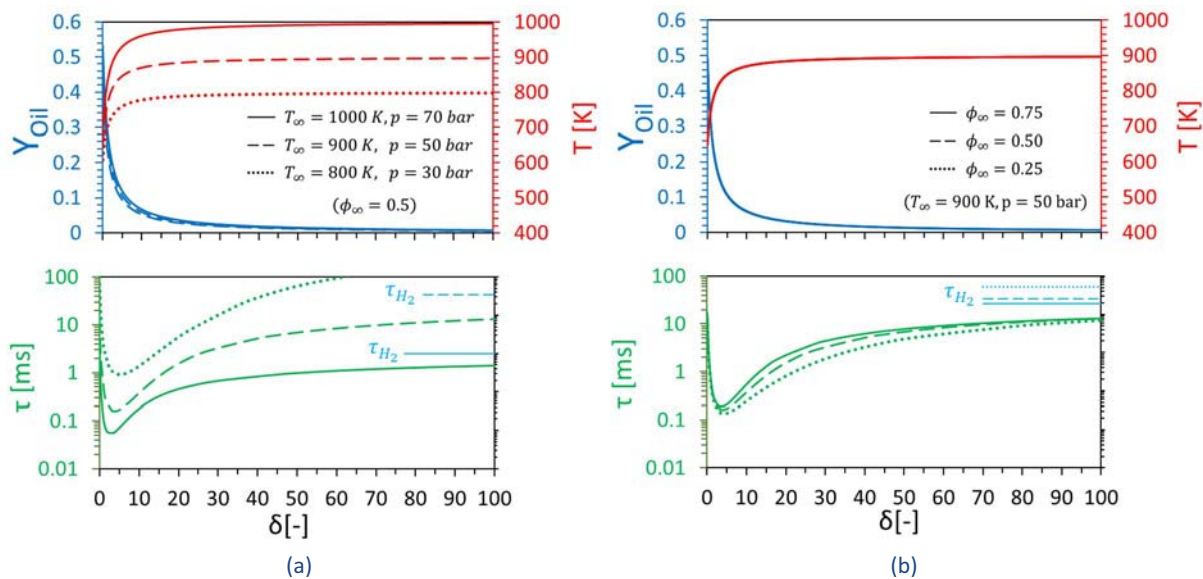


Figure 5. Mass fraction,  $Y_{oil}(\delta)$  and temperature,  $T(\delta)$  distributions obtained from the analytical model, together with ignition delay time distributions,  $\tau(\delta)$ , obtained from the OD simulations. Results obtained with  $\phi_{\infty} = 0.5$  for three different pressures and temperatures (a). Results obtained at  $T_{\infty} = 900$  K,  $p = 50$  bar for 3 different ambient equivalent ratios (b).

Finally, Figure 5 (b) shows that the extension of the region with very short values of  $\tau$  increases with the decrease of the ambient equivalence ratio. Considering that a comparable minimum value of  $\tau$  is obtained for the three cases (i.e., about 0.18 ms), the leanest case (i.e.,  $\phi_{\infty} = 0.25$ ) looks the most dangerous one. Such a result needs to be taken under particular consideration in the light of the development direction of hydrogen ICEs oriented towards lean operating combustion modes.

## 5. Conclusions

The analysis conducted in the present work had the aim of ascertaining if a lubricant oil droplet can promote undesired self-ignition of the charge in hydrogen Internal Combustion Engines (ICEs). Namely, a one-dimensional analytical model was coupled with the OpenSMOKE++ open-source chemical code with the purpose of assessing ignition delay variations of the charge induced by the presence of oil vapour. The analytical model was developed to derive reasonable thermo-chemical conditions in the vicinity of a vaporizing lubricant oil droplet, while the latter is suspended in a  $H_2/air$  environment in which engine-like conditions reign. The obtained results were used as input parameters for performing zero-dimensional numerical simulations in the OpenSMOKE++ framework. A single surrogate chemical species was employed to model the chemical and physical behaviour of lubricant oil, namely, n-hexadecane ( $n-C_{16}H_{34}$ ). A reduced chemical model, developed in a previous work for emulating the reactivity properties of  $H_2/n-C_{16}H_{34}/air$  mixtures, was used in the chemical kinetic simulations.

The results clearly confirmed that the oil vapour significantly increases the charge reactivity. It was found that the charge ignition delay reaches a minimum in the region close to the droplet surface, where its value can be reduced by up to two orders of magnitude, independently of the droplet radius and the equivalence ratio of the  $H_2/air$  mixture surrounding the droplet. Such a behaviour has been observed also in thermodynamic conditions that would not allow hydrogen to ignite. The reason relies on the low-temperature chemistry involved in the oxidation of long straight-chained alkanes constituting lubricant oil. This might explain how certain abnormal combustion modes can arise in hydrogen ICEs even in the absence of any significant charge or temperature inhomogeneity.

Despite the relative simplicity of the model employed in the calculations, it was possible to provide an answer to the question posed in the title via a practical approach that required limited computational efforts. The potentially harmful influence that lubricant oil might have on combustion regularity in hydrogen ICEs has been unveiled, with the results suggesting that an oil droplet can effectively serve as

a “sensitive” spot able to initiate an undesired ignition event that can potentially propagate to the remainder of the charge. Having assessed the importance of studying the fuel-lubricant interaction, more accurate calculations as well as experimental campaigns (also including secondary paths by which lubricant oil can interfere with the combustion process) might be now performed in order to provide more insight on the issue and accelerate the development of hydrogen combustion technology for ICEs.

## References

- [1] Robertson D, Prucka R. A Review of Spark-Assisted Compression Ignition (SACI) Research in the Context of Realizing Production Control Strategies. SAE Tech Pap 2019-24-0027 2019.
- [2] Paykani A, Kakaee A-H, Rahnama P, Reitz RD. Progress and recent trends in reactivity-controlled compression ignition engines. *Int J Engine Res* 2016;17:481–524.
- [3] Toulson E, Schock HJ, Attard WP. A Review of Pre-Chamber Initiated Jet Ignition Combustion Systems. SAE Tech Pap Ser 2010;1. <https://doi.org/10.4271/2010-01-2263>.
- [4] Distaso E, Amirante R, Cassone E, De Palma P, Sementa P, Tamburrano P, et al. Analysis of the Combustion Process in a Lean-Burning Turbulent Jet Ignition Engine Fueled with Methane. *Energy Convers Manag* 2020;223:113257.
- [5] Distaso E, Amirante R, Cassone E, Catapano F, De Palma P, Sementa P, et al. Experimental and Numerical Analysis of a Pre-Chamber Turbulent Jet Ignition Combustion System. SAE Tech Pap 2019-24-0018 2019.
- [6] Di Mauro A, Chen H, Sick V. Neural network prediction of cycle-to-cycle power variability in a spark-ignited internal combustion engine. *Proc Combust Inst* 2019;37:4937–44.
- [7] Ravaglioli V, Ponti F, De Cesare M, Stola F, Carra F, Corti E. Combustion Indexes for Innovative Combustion Control. *SAE Int J Engines* 2017;10:2371–81.
- [8] Kuronita T, Sakai T, Queck D, Puts R, Visser S, Herrmann O, et al. A Study of Dynamic Combustion Control for High Efficiency Diesel Engine. SAE Tech Pap 2020-01-0297 2020.
- [9] Amirante R, Casavola C, Distaso E, Tamburrano P. Towards the Development of the In-Cylinder Pressure Measurement Based on the Strain Gauge Technique for Internal Combustion Engines. SAE Tech Pap 2015-24-2419 2015.
- [10] Ashok B, Ashok SD, Kumar CR. A review on control system architecture of a SI engine management system. *Annu Rev Control* 2016;41:94–118.
- [11] Amirante R, Coratella C, Distaso E, Rossini G, Tamburrano P. Optical device for measuring the injectors opening in common rail systems. *Int J Automot Technol* 2017;18:729–42.
- [12] Eckerle W, Sujun V, Salemme G. Future Challenges for engine manufacturers in view of future emissions legislation. SAE Tech Pap 2017-01-1923 2017. <https://doi.org/https://doi.org/10.4271/2017-01-1923>.
- [13] Amirante R, Distaso E, Tamburrano P, Reitz RD. Laminar Flame Speed Correlations for Methane, Ethane, Propane and their Mixtures, and Natural Gas and Gasoline for Spark-Ignition Engine Simulations. *Int J Engine Res* 2017;18:951–70.
- [14] Hosseini SE, Butler B. An overview of development and challenges in hydrogen powered vehicles. *Int J Green Energy* 2020;17:13–37.
- [15] Faizal M, Chuah LS, Lee C, Hameed A, Lee J, Shankar M, et al. Review of hydrogen fuel for internal combustion engines. *J Mech Eng Res Dev* 2019;42:35–46.
- [16] Yip HL, Srna A, Yuen ACY, Kook S, Taylor RA, Yeoh GH, et al. A review of hydrogen direct injection for internal combustion engines: Towards carbon-free combustion. *Appl Sci* 2019;9:1–30. <https://doi.org/10.3390/app9224842>.
- [17] Xu H, Ni X, Su X, Xiao B, Luo Y, Zhang F, et al. Experimental and numerical investigation on effects of pre-ignition positions on knock intensity of hydrogen fuel. *Int J Hydrogen Energy* 2021;46:26631–45.
- [18] Aggarwal SK, Awomolo O, Akber K. Ignition characteristics of heptane-hydrogen and heptane-methane fuel blends at elevated pressures. *Int J Hydrogen Energy* 2011;36:15392–402. <https://doi.org/10.1016/j.ijhydene.2011.08.065>.
- [19] Wang FC-Y, Zhang L. Chemical composition of group II lubricant oil studied by high-resolution gas chromatography and comprehensive two-dimensional gas chromatography. *Energy&Fuels* 2007;21:3477–83.
- [20] Zaccardi J-M, Escudié D. Overview of the main mechanisms triggering low-speed pre-ignition in spark-ignition engines. *Int J Engine Res* 2015;16:152–65.
- [21] Wang Z, Liu H, Reitz RD. Knocking combustion in spark-ignition engines. *Prog Energy Combust Sci* 2017;61:78–112.
- [22] Distaso E, Amirante R, Calò G, De Palma P, Tamburrano P, Reitz RD. Investigation of Lubricant Oil influence on Ignition of Gasoline-like Fuels by a Detailed Reaction Mechanism. *Energy Proc* 2018;148:663–70.
- [23] Amann M, Alger T. Lubricant reactivity effects on gasoline spark ignition engine knock. *SAE Int J Fuels Lubr* 2012;5:760–71.
- [24] Gao J, Wang X, Song P, Tian G, Ma C. Review of the backfire occurrences and control strategies for port hydrogen injection internal combustion engines. *Fuel* 2022;307:121553. <https://doi.org/10.1016/j.fuel.2021.121553>.
- [25] Rouleau L, Duffour F, Walter B, Kumar R, Nowak L. Experimental and Numerical Investigation on Hydrogen Internal Combustion Engine. SAE TechPapers 2021. <https://doi.org/10.4271/2021-24-0060>.
- [26] Amirante R, Distaso E, Napolitano M, Tamburrano P, Iorio SD, Sementa P, et al. Effects of lubricant oil on particulate emissions from port-fuel and direct-injection spark-ignition engines. *Int J Engine Res* 2017;18:606–20.

- [27] Amirante R, Distaso E, Di Iorio S, Pettinicchio D, Sementa P, Tamburrano P, et al. Experimental Investigations on the Sources of Particulate Emission within a Natural Gas Spark-Ignition Engine. SAE Tech Pap 2017-24-0141 2017.
- [28] Distaso E, Amirante R, Calò G, De Palma P, Tamburrano P. Evolution of Soot Particle Number, Mass and Size Distribution along the Exhaust Line of a Heavy-Duty Engine Fueled with Compressed Natural Gas. *Energies* 2020;13:3993.
- [29] Distaso E, Amirante R, Tamburrano P, Reitz RD. Steady-state Characterization of Particle Number Emissions from a Heavy-Duty Euro VI Engine Fueled with Compressed Natural Gas. *Energy Proc* 2018;148:671–8.
- [30] Amirante R, Distaso E, Di Iorio S, Sementa P, Tamburrano P, Vaglieco BM, et al. Effects of natural gas composition on performance and regulated, greenhouse gas and particulate emissions in spark-ignition engines. *Energy Convers Manag* 2017;143:338–47.
- [31] Distaso E, Amirante R, Tamburrano P, Reitz RD. Understanding the role of soot oxidation in gasoline combustion: A numerical study on the effects of oxygen enrichment on particulate mass and number emissions in a spark-ignition engine. *Energy Convers Manag* 2019;184:24–39.
- [32] Huang Y, Li Y, Zhang W, Meng F, Guo Z. 3D simulation study on the influence of lubricant oil droplets on pre-ignition in turbocharged DISI engines. *Proc Inst Mech Eng Part D J Automob Eng* 2018;232:1677–93.
- [33] Ohtomo M, Suzuoki T, Miyagawa H, Koike M, Yokoo N, Nakata K. Fundamental analysis on auto-ignition condition of a lubricant oil droplet for understanding a mechanism of low-speed pre-ignition in highly charged spark-ignition engines. *Int J Engine Res* 2019;20:292–303.
- [34] Distaso E, Amirante R, Calò G, De Palma P, Tamburrano P. Lubricant-Oil-Induced Pre-ignition Phenomena in Modern Gasoline Engines: Using Experimental Data and Numerical Chemistry to Develop a Practical Correlation. SAE Tech Pap 2021-24-0052 2021.
- [35] Gupta A, Shao H, Remias J, Roos J, Wang Y, Long Y, et al. Relative Impact of Chemical and Physical Properties of the Oil-Fuel Droplet on Pre-Ignition and Super-Knock in Turbocharged Gasoline Engines. 2016.
- [36] Distaso E, Amirante R, Calò G, De Palma P, Tamburrano P, Reitz RD. Predicting Lubricant Oil Induced Pre-Ignition Phenomena in Modern Gasoline Engines: the Reduced GasLube Reaction Mechanism. *Fuel* 2020;281:118709.
- [37] Palaveev S, Magar M, Kubach H, Schiessl R, Spicher U, Maas U. Premature flame initiation in a Turbocharged DISI engine - Numerical and experimental investigations. *SAE Int J Engines* 2013;6:54–66.
- [38] Kuti OA, Yang SY, Hourani N, Naser N, Roberts WL, Chung SH, et al. A fundamental investigation into the relationship between lubricant composition and fuel ignition quality. *Fuel* 2015;160:605–13.
- [39] Distaso E, Calò G, Amirante R, De Palma P, Mehl M, Pelucchi M, et al. Highlighting the Role of Lubricant Oil in the Development of Hydrogen Internal Combustion Engines by means of a Kinetic Reaction Model. *J. Phys. Conf. Ser.*, vol. 2385, 2022, p. 12078.
- [40] Zhang H, Law CK. Effects of temporally varying liquid-phase mass diffusivity in multicomponent droplet gasification. *Comb Flame* 2008;153:593–602.
- [41] Law CK, Williams FA. Kinetics and convection in the combustion of alkane droplets. *Comb Flame* 1972;19:393–405.
- [42] Snegirev AY. Transient temperature gradient in a single-component vaporizing droplet. *Int J Heat Mass Transf* 2013;65:80–94.
- [43] Monogenidou SA, Assael MJ, Huber ML. Reference Correlation for the Thermal Conductivity of n-Hexadecane from the Triple Point to 700 K and up to 50 MPa. *J Phys Chem Ref Data* 2018;47:13103.
- [44] Abramenko TN, Aleinikova VI, Golovicher LE, Kuz'mina NE. Generalization of experimental data on thermal conductivity of nitrogen, oxygen, and air at atmospheric pressure. *J Eng Phys Thermophys* 1992;63:892–7.
- [45] Bergman TL, Bergman TL, Incropera FP, Dewitt DP, Lavine AS. *Fundamentals of heat and mass transfer*. John Wiley & Sons; 2011.
- [46] Mathur S, Tondon PK, Saxena SC. Thermal conductivity of binary, ternary and quaternary mixtures of rare gases. *Mol Phys* 1967;12:569–79.
- [47] Zhukov VP, Pätz M. On thermal conductivity of gas mixtures containing hydrogen. *Heat Mass Transf* 2017;53:2219–22.
- [48] Haynes WM. *CRC handbook of chemistry and physics*. CRC press; 2016.
- [49] Johnson BT, Hargrave GK, Reid BA, Page VJ, others. *Optical analysis and measurement of crankcase lubricant oil atomisation*. 2012.
- [50] Wang Z, Zhang D, Fang Y, Song M, Gong Z, Feng L. Experimental and numerical investigation of the auto-ignition characteristics of cylinder oil droplets under low-speed two-stroke natural gas engines in-cylinder conditions. *Fuel* 2022;329:125498.
- [51] Cuoci A, Mehl M, Buzzi-Ferraris G, Faravelli T, Manca D, Ranzi E. Autoignition and burning rates of fuel droplets under microgravity. *Comb Flame* 2005;143:211–26.
- [52] Thirouard B, Tian T. Oil transport in the piston ring pack (Part I): identification and characterization of the main oil transport routes and mechanisms. 2003.
- [53] Long Y, Wang Z, Qi Y, Xiang S, Zeng G, Zhang P, et al. Effect of Oil and Gasoline Properties on Pre-Ignition and Super-Knock in a Thermal Research Engine (TRE) and an Optical Rapid Compression Machine (RCM). 2016.
- [54] Cuoci A, Frassoldati A, Faravelli T, Ranzi E. OpenSMOKE++: An object-oriented framework for the numerical modeling of reactive systems with detailed kinetic mechanisms. *Comput Phys Commun* 2015;192:237–64.